Available online at www.sciencedirect.com
ScienceDirect
International Journal of Thermal Sciences 46 (2007) 399–406
International Journal of Thermal Sciences
www.elsevier.com/locate/ijts

Numerical investigation on optical and heat transfer characteristics of a rapid thermal annealing system for LCD manufacturing

S.H. Lee [a], D.H. Shin [b], H.J. Kim [c], S. Park [d], J.S. Lee [e,*]

[a] *School of Mechanical Engineering, Chung-Ang University, Seoul 156-756, Republic of Korea*
[b] *Viatron Technologies Inc., Seoul 153-803, Republic of Korea*
[c] *School of Chemical System Engineering & Advanced Materials, Hongik University, Seoul 121-791, Republic of Korea*
[d] *Department of Mechanical & System Design Engineering, Hongik University, Seoul 121-791, Republic of Korea*
[e] *School of Mechanical & Aerospace Engineering, Seoul National University, Seoul 151-742, Republic of Korea*

Received 24 January 2006; received in revised form 16 June 2006; accepted 20 June 2006

Available online 14 August 2006

Abstract

The objectives of present study are to propose a method to evaluate the quality of polycrystalline silicon film by using the thin film optics analysis, and to investigate heat transfer characteristics in a rapid thermal annealing system for liquid crystal display (LCD) manufacturing. The transmittance of polycrystalline silicon film is calculated by the characteristic transmission matrix method, and predicted results are compared with the experimental data for two different samples. The transient one-dimensional conduction and radiation heat transfer equations are additionally solved to predict the surface temperature of thin films. The two-flux method is employed to evaluate radiation heat transfer, and the ray-tracing method is utilized to take into account of the wave interference effect. As the film thickness increases, the peak transmittance value increases and the wavelength where the peak appears becomes longer due to wave interference. These characteristics can be used for *in situ* and practical estimation of the extent of crystallization of the silicon film during the process. From the thermal analysis, it is shown that the selective heating in the multilayer film structure acts as an important mechanism during the annealing of silicon film deposited on the glass.

Keywords: Crystallization; Annealing; Liquid crystal display (LCD); Optics; Heat transfer; Wave interference

1. Introduction

Recently, a new type of display technology has gained a lot excitement in the OLED (Organic Light Emitting Diode) displays industry. The OLED displays are being hailed as the next big wave, and they require polycrystalline silicon (poly-Si) backplanes. This trend leads many academic institutions and industry leaders to be intensively trying to develop new technologies for cost-effective mass-production of poly-Si substrates with high quality. A new technology, so-called field-enhanced rapid thermal annealing (FE-RTA), has been developed by Viatron Technologies, Inc. [1]. This makes it possible to yield the poly-Si films with better quality in a more cost-effective manner.

Two key-issues are indeed confronted in designing the RTA system. The first issue is how to evaluate the quality of a polycrystalline silicon film in a quantitative way. Several non-contact methods such as photograph, ultraviolet spectrometers, and Raman shift have been used in qualitatively evaluating the extent of crystallization. However, for a more accurate evaluation, a quantitative method is required. The present study thus proposes a way to estimate about how good or bad the silicon films are from a thin film optics simulation. This method is based on the fact that the optical features between amorphous and crystalline silicon lattice structures are different from each other. By the characteristic transmission matrix method, the transmittance in multilayer thin film structure is estimated, and compared with the experimental data measured by the

* Corresponding author. Tel.: +82 2 880 7117; fax: +82 2 883 0179.
E-mail address: jslee123@snu.ac.kr (J.S. Lee).

1290-0729/$ – see front matter
doi:10.1016/j.ijthermalsci.2006.06.009

Nomenclature

a_λ	spectral absorption coefficient $(= 4\pi\kappa/\lambda)$	cm^{-1}
C_p	heat capacity	$J\,kg^{-1}\,K^{-1}$
c_0	speed of light in vacuum	$m\,s^{-1}$
d	film thickness	m
h	Planck constant $(= 6.6262 \times 10^{-34}$ J s)	J s
i	unit of imaginary number	
i_λ^+	spectral radiative intensity in the positive z direction	$W\,m^{-2}\,\mu m^{-1}\,sr^{-1}$
i_λ^-	spectral radiative intensity in the negative z direction	$W\,m^{-2}\,\mu m^{-1}\,sr^{-1}$
$i_{\lambda b}$	spectral blackbody radiative intensity	$W\,m^{-2}\,\mu m^{-1}\,sr^{-1}$
k	thermal conductivity	$W\,m^{-1}\,K^{-1}$
k_B	Boltzmann constant $(= 1.380658 \times 10^{-23}\,J\,K^{-1})$	$J\,K^{-1}$
M	characteristic transmission matrix	
N	number of layers	
n	simple refractive index	
$\tilde{n}$	complex refractive index	
q_r	radiative heat flux	$W\,m^{-2}$
r_F	Fresnel reflection coefficient	
R	reflectance of lumped structure	
t_F	Fresnel transmission coefficient	
T	temperature (K) or transmittance	
z	coordinate	

Greek symbols

θ	angle	rad
$\tilde{\theta}$	complex angle of incidence	
κ	extinction coefficient	cm^{-1}
κ_λ	optical depth	
λ	wavelength	μm
μ	directional cosine	
ρ	density or interfacial reflectivity	$kg\,m^{-3}$
ψ	fraction representing the extent of crystallization	

Subscripts

aSi	amorphous silicon
cSi	crystalline silicon
i	incident
m	layer index
poly	polycrystalline silicon

ultraviolet-spectrometer [1]. Besides, the film thickness effect on transmittance is examined.

The second issue is how to predict the film surface temperature during the rapid thermal annealing process. *In situ* measurement of poly-Si film temperature is practically impossible in most RTA systems, because of very narrow space for probing in the RTA system where the moving tray is located. In order to design more efficient RTA systems, a thermal analysis becomes essential, and for a more accurate analysis, the radiative energy transfer should be coupled with the thin film optics analysis for silicon films.

The present study predicts the film surface temperature by considering the transient one-dimensional conduction and radiation heat transfer. The two-flux model is used to calculate the spectral radiation intensities, and the ray tracing method is taken to describe the wave interference effect appearing in the thin film structure. The issues raised above are obviously very important for thermal design of RTA systems in manufacturing LCD backplanes with better quality. The present study is believed to provide useful information on thermal/optical characteristics for more efficient RTA systems.

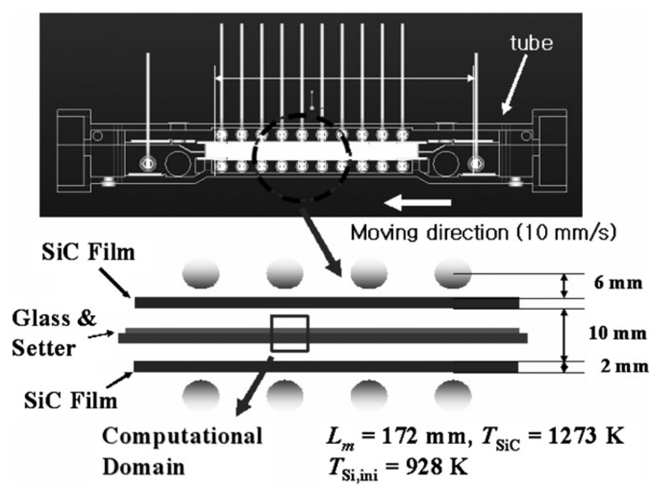

Fig. 1. Schematic of RTA system.

2. Analysis

2.1. Thin film optics simulation

The thin film optics simulation is conducted to evaluate the extent of crystallization of silicon films during the process. In the simulation, lumped optical characteristics of the multilayer thin film structure are analyzed by the characteristic transmission matrix method [2] considering the wave interference effect that might be present in thin film structures. Fig. 1 shows the multilayer thin film structure to be considered. The characteristic transmission matrix of the mth layer is expressed on the basis of s-polarized light, i.e., TE (transverse electric), as follows:

$$M_m(z) = \begin{bmatrix} M_{11} & M_{12} \\ M_{21} & M_{22} \end{bmatrix}_m = \begin{bmatrix} \cos(\frac{2\pi}{\lambda}\tilde{p}_m z_m) & -\frac{i}{\tilde{p}_m}\sin(\frac{2\pi}{\lambda}\tilde{p}_m z_m) \\ -i\,\tilde{p}_m \sin(\frac{2\pi}{\lambda}\tilde{p}_m z_m) & \cos(\frac{2\pi}{\lambda}\tilde{p}_m z_m) \end{bmatrix} \tag{1}$$

where $\tilde{p}_m = \tilde{n}_m \cos\tilde{\theta}_m$. $\tilde{\theta}_m$ denotes the complex angle of incidence and can be acquired from the generalized Snell's law, which is given by $\sin\theta_i = \tilde{n}_m \sin\tilde{\theta}_m$. The complex refractive index is defined as $\tilde{n} = n - i\kappa$ where both n and κ depend on the wavelength. Then, the multilayer transmission matrix, M, can be expressed as follows:

$$M = \begin{bmatrix} M_{11} & M_{12} \\ M_{21} & M_{22} \end{bmatrix} = \prod_{m=1}^{N} M_m(z) \tag{2}$$

where N is the total number of layers. The reflection and transmission coefficients can be obtained from the following formulae:

$$r_F = \frac{(M_{11} + M_{12}\tilde{p}_{N+1})\tilde{p}_0 - (M_{21} + M_{22}\tilde{p}_{N+1})}{(M_{11} + M_{12}\tilde{p}_{N+1})\tilde{p}_0 + (M_{21} + M_{22}\tilde{p}_{N+1})} \tag{3}$$

$$t_F = \frac{2\tilde{p}_0}{(M_{11} + M_{12}\tilde{p}_{N+1})\tilde{p}_0 + (M_{21} + M_{22}\tilde{p}_{N+1})} \tag{4}$$

From Eqs. (3) and (4), the lumped structure reflectance and transmittance can be determined as follows:

$$R = |r_F|^2 \tag{5a}$$

$$T = \frac{\tilde{p}_{N+1}}{\tilde{p}_0}|t_F|^2 \tag{5b}$$

For considering both TE and TM waves, the corresponding formulae for the TM wave can immediately be obtained from Eqs. (3)–(5) by replacing the quantities $\tilde{p}_0$ and $\tilde{p}_{N+1}$ by

$$\tilde{q}_0 = \cos\tilde{\theta}_0/\tilde{n}_0 \tag{6a}$$

$$\tilde{q}_{N+1} = \cos\tilde{\theta}_{N+1}/\tilde{n}_{N+1} \tag{6b}$$

respectively, on the assumption that all the media are nonmagnetic.

2.2. Conduction and radiation heat transfer

In addition to the optical analysis, another purpose of this study is to investigate thermal characteristics in the RTA system for the LCD manufacturing process. As shown in Fig. 2, the RTA system is composed of two SiC films to emit the radiative energy in the near infrared spectrum, and a series of halogen lamps. The amorphous silicon film deposited on the glass (SiO_2) film enters the RTA system and moves along the setter which is made of quartz. As the rapid thermal annealing progresses, the amorphous silicon film becomes the polycrystalline one for LCD panels. When the multilayer film structure enters the RTA system, it is heated up to 928 K in the preliminary stage. Here, conduction and radiation heat transfer plays a dominant role in the annealing process of the amorphous film. In particular, the radiative heat transfer is highly affected by the opto-thermal properties varying with wavelengths. Thus, it is necessary to combine the present thermal analysis with the thin film optics simulations. The present study approximates one-dimensional energy transfer passing through the films because of very short distance between two SiC films and large aspect ratios of films. Since the quartz tray is moving with time from right to left, transient phenomena is included by applying the appropriate boundary conditions to both ends of the multilayer thin film structure.

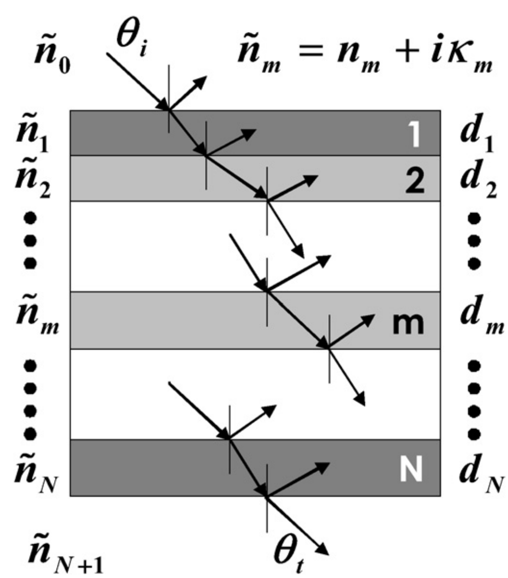

Fig. 2. Schematic of multilayered thin film structure.

The one-dimensional transient conduction and radiation equation is given by

$$\rho C_P \frac{\partial T}{\partial t} = \frac{\partial}{\partial z}\left(k\frac{\partial T}{\partial z}\right) - \frac{\mathrm{d}q_r}{\mathrm{d}z} \tag{7}$$

where q_r is the total radiative heat flux integrated over all wavelengths. The convective heat transfer is ignored because the heat transfer rate by convection is much smaller than other heat transfer modes.

Without scattering, the divergence of radiation heat flux can be expressed in the context of the two-flux model as [3]

$$\frac{\mathrm{d}q_r(z)}{\mathrm{d}z} = \frac{\mathrm{d}}{\mathrm{d}z}\left\{\pi\int_0^\infty \left[i_\lambda^+(\kappa_\lambda,\mu) - i_\lambda^-(\kappa_\lambda,\mu)\right]\mathrm{d}\lambda\right\} \tag{8}$$

where the direction cosine $\mu = \cos\theta$, and i_λ^+ and i_λ^- are spectral radiation intensities directed to positive ($0 \leqslant \theta \leqslant \pi/2$) and negative ($\pi/2 \leqslant \theta \leqslant \pi$) directions, respectively. Meanwhile, the optical depth κ_λ in Eq. (8) is defined as

$$\kappa_\lambda = \int_0^z a_\lambda(z')\,\mathrm{d}z' \tag{9}$$

where $a_\lambda(z)$ is the spectral absorption coefficient. The radiative transfer equation for the upward and downward intensities can be written as

$$\mu\frac{\mathrm{d}i_\lambda^+}{\mathrm{d}z} = -a_\lambda(z)\left[i_\lambda^+(z) - i_{\lambda b}(z)\right], \quad \text{for } 0 \leqslant \theta \leqslant \frac{\pi}{2} \tag{10a}$$

$$\mu\frac{\mathrm{d}i_\lambda^-}{\mathrm{d}z} = -a_\lambda(z)\left[i_\lambda^-(z) - i_{\lambda b}(z)\right], \quad \text{for } \frac{\pi}{2} \leqslant \theta \leqslant \pi \tag{10b}$$

where $i_{\lambda b}$ is the blackbody spectral intensity, which is given by the Planck's law as follows:

$$i_{\lambda b}(z) = \frac{2n^2 C_1}{\lambda^5(e^{C_2/\lambda T(z)} - 1)} \tag{11}$$

where $C_1 = hc_0^2$ and $C_2 = hc_0/k_B$. In general, the refractive index n is dependent on the wavelength.

2.3. Computational details

From the proceeding discussion, it is evident that there are two issues involved that should be addressed; evaluation method for the extent of crystallization, and thermal analysis. At first, as expressed in Eqs. (1)–(6), the characteristic transmission matrix method is solely utilized for the estimation of transmittance and reflectance. In this case, thermal analysis is excluded because the present study is mainly devoted to propose a method for the evaluation of the optical characteristics of multilayer thin film structures. For conduction and radiation heat transfer analysis, an implicit finite-difference method is used to integrate transient and spatial terms in Eqs. (7), (8), and (10). The Neumann boundary conditions are imposed at $z = 0$ and $z = d_1 + d_2 + d_3$ in the thermal analysis.

For radiative heat transfer, the incident radiation intensities at the front and back surfaces are assumed to follow Planck's spectral distribution as given in Eq. (11). As illustrated in Fig. 3, the interfacial reflectance and transmittance between two dissimilar materials are determined for various wavelengths from Fresnel relations [3]. Consider a plane wave propagating through a non-absorbing air that is incident on multilayered absorbing films (polycrystalline silicon, SiO_2, and glass) as shown in Fig. 3. At the first interface, part of the energy, $\rho_\lambda^+ i_\lambda^+$, is reflected and the rest, $(1 - \rho_\lambda^+) i_\lambda^+$, is transmitted through the interface. The transmitted energy decays exponentially by absorption as the wave propagates through the films. Similarly, part of the transmitted energy that reaches the second interface is converted into reflected energy, and the rest is transmitted into the absorbing substrate. The energy that is trapped inside the film will be reflected forth and back until it is either absorbed in the film or transmitted out. For both TE and TM waves, the Fresnel coefficients including interference are used to determine interfacial reflectivity and transmissivity, and by using the ray-tracing method, the contributions from all the multiple reflections can be evaluated with wave interference effects.

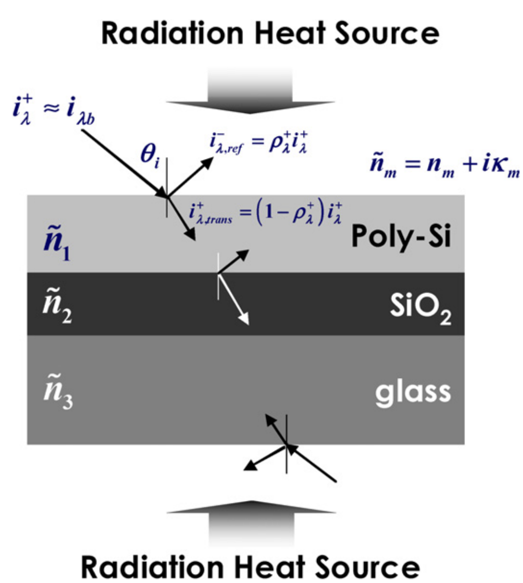

Fig. 3. Schematic of poly-silicon thin film structure.

The initial film temperature is set at 928 K that is heated up in the preliminary stage. The adopted time step and mesh size used for each simulation are determined through grid- and time-dependence tests. The thermal/optical calculations are repeated for each time step until the convergence criterion is satisfied. The final solutions are obtained when the relative deviation of temperature and radiative intensity is less than 10^{-4}, and the residuals from conduction equation are likewise less than 10^{-3}.

3. Results and discussion

3.1. Optical characteristics

First, optical characteristics are analyzed considering the wave interference, which takes place in the multilayer thin film structure as depicted in Fig. 3. The transmission matrix method enables to predict the dependence of lumped structure transmission, reflectance, and absorptance on wavelengths. It is crucial to understand the optical features of the multilayer thin film structure because radiation energy transfer is significantly affected by the behavior of lights propagating through the medium. To simulate the optical characteristics, the optical coefficients of solids should be given for amorphous silicon, crystalline silicon, silicon dioxide (glass), and quartz. These optical constants are taken from references [4–6], e.g., refractive index and extinction coefficient shown in Figs. 4 and 5. To evaluate the extent of crystallization of the silicon film, the weighted forms of refractive index and extinction coefficient are defined for the polycrystalline silicon film as follows:

$$n_{poly} = \psi n_{aSi} + (1 - \psi) n_{cSi} \tag{12a}$$

$$\kappa_{poly} = \psi \kappa_{aSi} + (1 - \psi) \kappa_{cSi} \tag{12b}$$

where ψ is the crystallization degree, indicating how much the film is crystallized during the annealing process. $\psi = 1.0$ means a 100% crystalline film, for instance, whereas $\psi = 0$ for a 100% amorphous state.

For transmittance of the lumped structure, numerical predictions are compared with experimental data measured by ultraviolet spectrometers [1]. Two samples of the poly-Si films prepared by two different methods are examined: one is manufactured by the typical RTA system, and the other is made by the new FE-RTA technology [1]. In the optical analysis, the wavelength region of interest ranges from 0.01 to 2 µm. Film thicknesses of poly-Si film, SiO_2, and quartz are 50 nm, 0.5 µm, and 700 µm, respectively.

The predicted transmittance behaviors are presented in Fig. 6 for the silicon film with 50 nm in thickness at different extents of crystallization, ψ. As the fraction ψ increases, the transmittance becomes larger in the visible spectrum. It means that the reflected waves at the interface are rarely absorbed in the medium in the case of the perfect crystalline silicon film because of relatively lower extinction coefficient compared to the amorphous silicon. The transmittance reaches a maximum value at 0.48 µm.

Fig. 7 shows comparison between predictions and measurements for two different samples, as mentioned previously. One

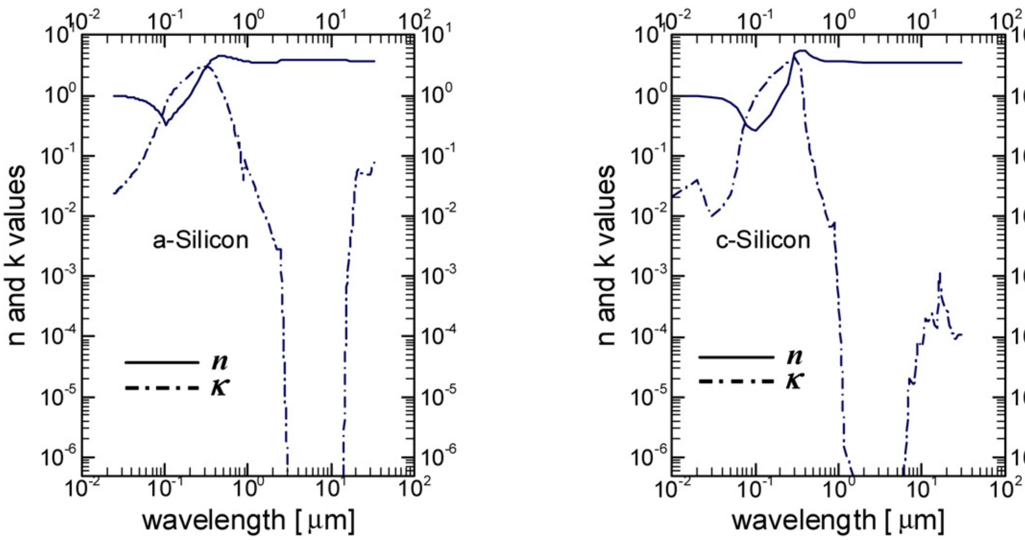

Fig. 4. Optical constants of amorphous and crystal silicon [6,7].

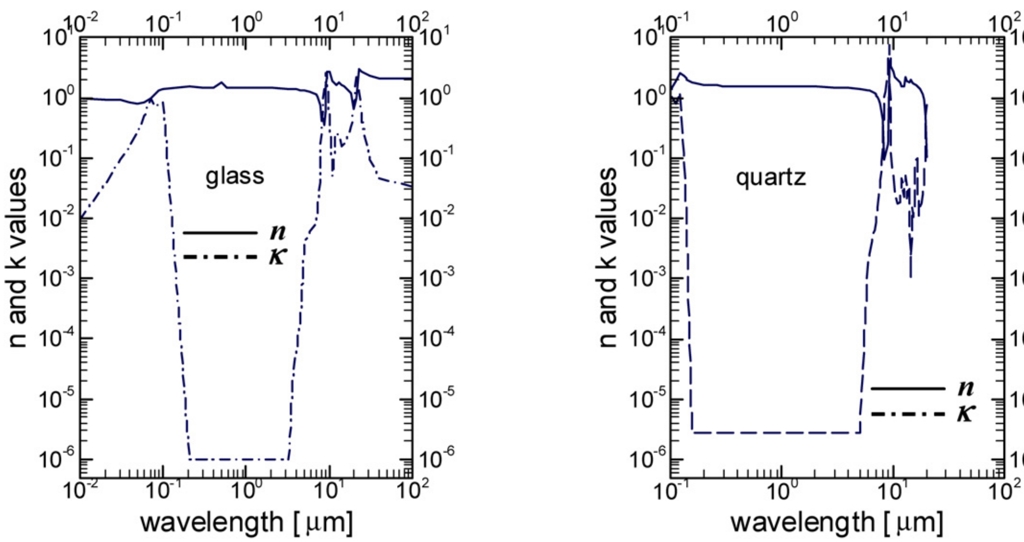

Fig. 5. Optical constants of SiO_2 (glass) and quartz [5].

of them is fabricated by the typical SPC (Solid Phase Crystallization) process, and the other is by the new FE-RTA technology. Experiments were extensively conducted by the ultraviolet spectrometer [1] for polycrystalline silicon films of 50 nm thickness. From the measured data for two samples, the polysilicon film processed by the FE-RTA shows better quality compared to that by the typical SPC process, that is, the maximum transmittance at about 0.46 μm obtained by the SPC process is about 50%, whereas it reaches up to 63% by the FE-RTA process. From comparison with predicted data, the silicon film manufactured by the FE-RTA process can be estimated to be within the extent of 96% crystalline.

The film thickness effect on the transmittance is depicted in Fig. 8. It is interesting to note that, in general, the maximum transmittance takes place at longer wavelengths as the film thickness is getting thicker. This fact indicates that such wavelength regions where the maximum transmittance takes place would be present in a deterministic way according to the film thickness. By controlling the wavelength in an appropriate manner, the maximum transmittance of a lumped structure could be achieved. It seems to be associated with the wave interference effect between incident and reflected waves in the medium. Both amorphous and crystalline silicons follow this tendency, but the increasing pattern appears more obviously in the perfect crystalline silicon film. Meanwhile, the maximum transmittance value increases with film thickness. It is obvious from Fig. 8(b) that the wavelength at maximum transmittance value is getting longer with increasing the film thickness, especially in the perfect crystalline silicon film because of lower extinction coefficient with an increase in the wavelength as can be seen in Fig. 4(b).

3.2. Heat transfer characteristics

It is assumed for simplicity that the blackbody radiation is emitted from the lamps. The wavelength range is taken from

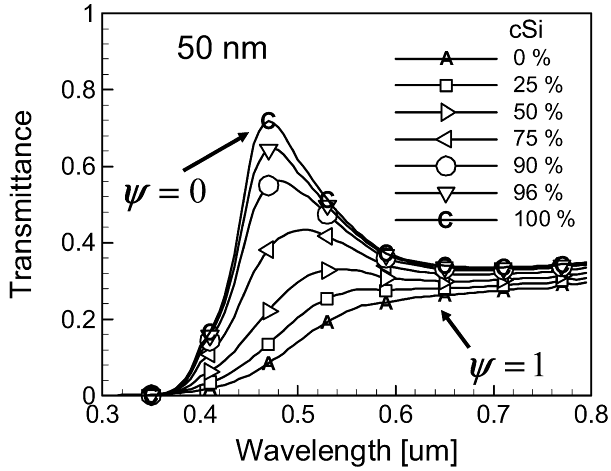

Fig. 6. Variation of transmittance with respect to wavelength for different degrees of crystallization.

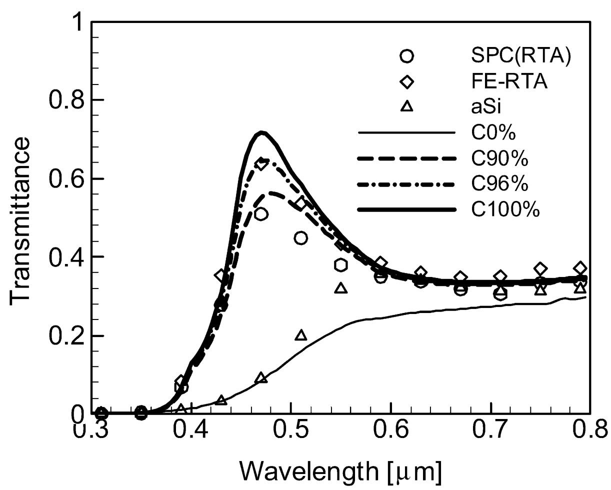

Fig. 7. Comparison of predicted transmittance with experimental data.

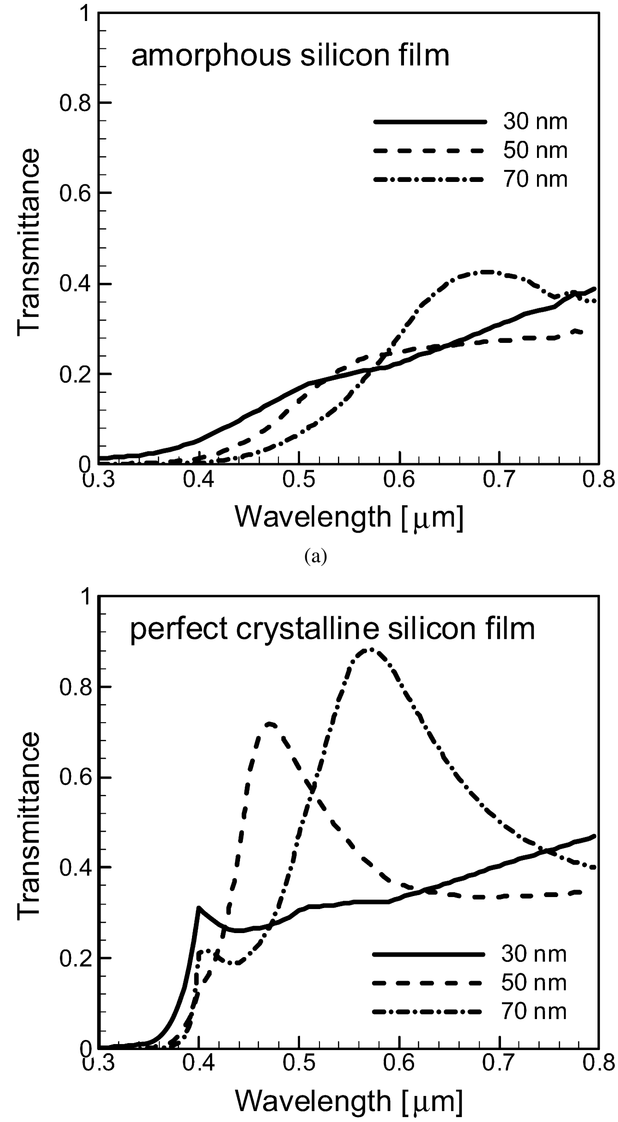

Fig. 8. Film thickness effect on transmittance for (a) amorphous silicon and (b) crystalline silicon.

0.01 μm to 20 μm in the simulation of thermal energy transfer, because hemispherical spectral emissive power in this range approaches 98% of the blackbody emissive power at a typical lamp temperature of 1000 K used in the present RTA system. In the thermal analysis, the finite difference method is used to solve the integro-differential type of Eqs. (7), (8), and (10). When the transmitting layer is so thin that its thickness is comparable to the radiation wavelength, there can be interference between incident and reflected waves. We use the ray-tracing method [3,7] to take into account of wave interference effects in the structure. In both positive and negative z directions, the calculations are repeated over and over until the relative errors between previous and current steps are less than 10^{-6}. Once the spectral radiative intensities are calculated, they are integrated over such a range of wavelength spectrum.

Fig. 9 shows the present one-dimensional grid system determined after the grid-dependence test performed in advance. The surface emissivity is obviously a critical parameter in the temperature control and thermal modeling of the RTA processing of semiconductors. The temperature-dependent emissivity of silicon has been studied by using different heating methods, including furnace [8,9], electron beam [10], and contact heating [9]. Chen and Borca-Tasciuc [11] investigated the photon effect on radiative properties of silicon during rapid thermal processing. Their study indicated that such a photon effect might impose a limit on the accuracy of the pyrometry method in the temperature measurement. Fortunately, the temperature range considered in the present study does not exceed 800 K where the emissivity remains nearly constant as 0.7, even when the temperature becomes higher than 800 K. As shown in Fig. 1, the total length is 172 mm and the scanning speed of tray is 10 mm s^{-1}. Thus, it can easily be shown that the total time is 17.2 s during which the multilayer structure undergoes the rapid heating process. Furthermore, SiC film temperature heated by lamps remains constant and its value is about 1273 K in the present simulation.

Fig. 10 illustrates total radiative heat flux distributions in the z direction. Two extreme cases, i.e., amorphous and perfect

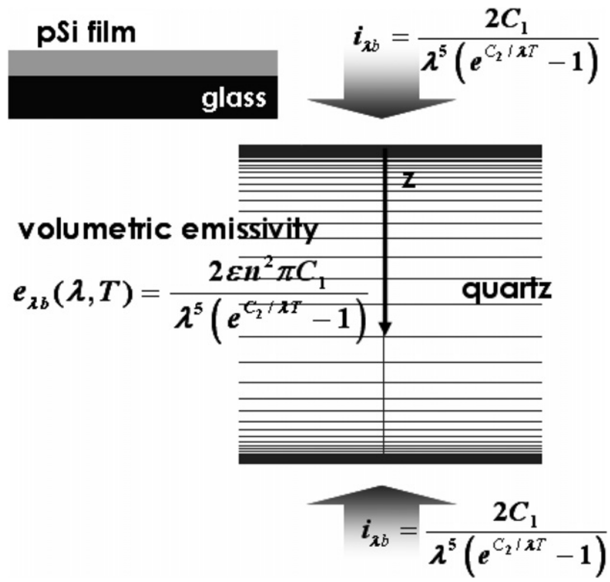

Fig. 9. Computational domain for heat transfer analysis.

crystalline silicon films are considered to easily figure out the distinctive thermal features during the annealing process. The spatial gradient of radiative heat flux for the amorphous silicon is larger than that for the perfect crystalline silicon. It indicates that the crystalline silicon film hardly absorbs the thermal radiation energy because its extinction coefficient is smaller than that of the amorphous silicon as shown in Fig. 4. The extinction coefficient of the amorphous silicon is indeed about 100 times as large as that of the crystalline silicon at $\lambda = 20$ μm. That is, most of radiation beams are transmitted through the crystalline silicon film. Thus, the transmittance value can be used as a measure of crystallization degree since the increase in transmittance implies that the silicon film structure is getting closer to the perfect crystalline one. On the contrary, the slope of radiative heat flux distributions in the SiO_2 (glass) region ($z > 50$ nm) is found to be higher compared to those of amorphous and perfect crystalline silicon films. This is due to larger absorption of radiation from lamps in this region because the extinction coefficient of SiO_2 is larger than that of the silicon film in the near-infrared region, as observed in Fig. 5. During the annealing process, such selective heating regions would be present in the glass film, resulting in the deposited silicon film to be heated up. At the interface between silicon and glass films, thermal conduction becomes dominant. In fact, about 75% of blackbody total emissive power at 1000 K is contained in the near-infrared region. In the visible region, most of radiation passes through the SiO_2 film, which, however, has much larger extinction coefficients in the spectral range from 8 to 20 μm. The selective heating occurs in the SiO_2 film because of the different spectral dependence of the extinction coefficient for each material. Thus, by controlling radiation spectrum irradiated on the multilayer thin film structure, more efficient thermal annealing process can be achieved.

The predicted surface temperatures for amorphous and perfect crystalline silicon films are presented in Fig. 11. As mentioned before, it is hardly possible to measure the surface temperature directly, because of very narrow space for probing

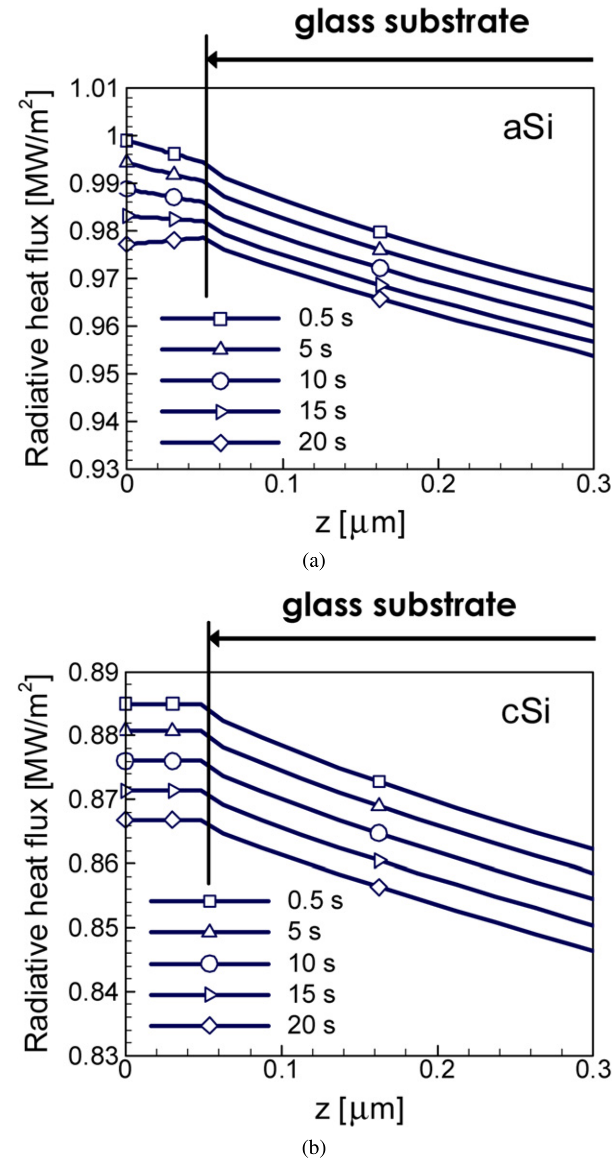

Fig. 10. Radiative heat flux distributions for (a) amorphous and (b) crystalline silicon films.

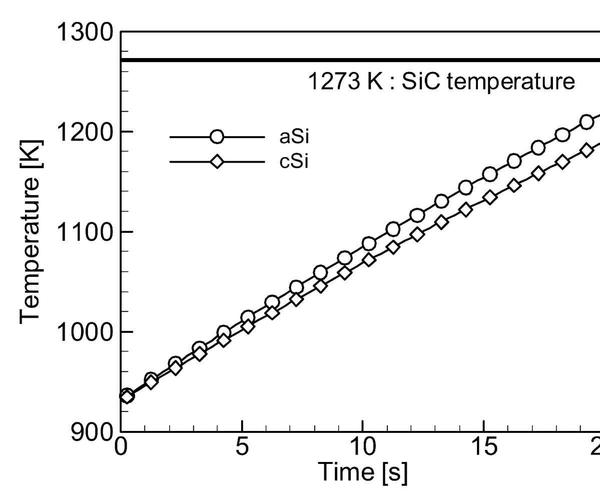

Fig. 11. Estimation of surface temperature history for amorphous and crystalline silicon films.

in the RTA system. In this respect, the prediction of the surface temperature may be helpful in designing and evaluating the present RTA system. At the lamp exposure time of 17 s, the heated surface temperatures are 1167 K and 1143 K for amorphous and crystalline silicon films, respectively. The temperature rise in the amorphous film is slightly faster than that in the crystalline silicon film simply because of larger absorption by amorphous film. Besides, from this calculation, the averaged heating rate of both cases is estimated to be 13.8 $\mathrm{K\,s^{-1}}$.

4. Conclusions

The thin film optics simulation is conducted to investigate the thermal characteristics of a multilayer thin film structure composed of a silicon thin film, an SiO_2 (glass) film, and quartz. Some important observations are noticed and summarized below.

(1) A new method is proposed to evaluate the quality of silicon films during the rapid thermal annealing process. As the crystallization progresses, the maximum transmittance of the lumped structure becomes larger. We examine two different samples by comparisons of predicted transmittance with the measured data. As a result, the polycrystalline silicon film produced by the new FE-RTA technology is evaluated better than that by the typical SPC process.
(2) As the film thickness increases, the maximum transmittance of lumped structure occurs at longer wavelengths. It indicates that such wavelength regions appear in deterministic patterns according to the film thickness. It is also found that the maximum values of transmittance increase with film thickness.
(3) The amorphous silicon film absorbs radiation energy much larger than the perfect crystalline silicon film does in the wavelength region of interest. Such selective heating effect appearing in SiO_2 film can serve to the thermal enhancement of the deposited silicon film. It contributes to accelerate the annealing process. It is found that the surface temperature is estimated to be in the range from 1143 K to 1167 K, and the averaged heating rate is about 13.8 $\mathrm{K\,s^{-1}}$.

Acknowledgements

The authors gratefully acknowledge financial support from the Micro Thermal System Research Center sponsored by the Korea Science and Engineering Foundation.

References

[1] http://www.viatrontech.com.
[2] M. Born, W. Wolf, Principles of Optics: Electromagnetic Theory of Propagation, Interference, and Diffraction of Light, sixth ed., Cambridge University Press, Cambridge, UK, 1980.
[3] R. Siegel, J.R. Howell, Thermal Radiation Heat Transfer, Taylor & Francis, Washington, DC, 1992.
[4] H.R. Philipp, in: E.D. Palik (Ed.), Handbook of Optical Constants of Solids, Academic Press, San Diego, 1998.
[5] H. Piller, in: E.D. Palik (Ed.), Handbook of Optical Constants of Solids, Academic Press, San Diego, 1998.
[6] D.F. Edwards, in: E.D. Palik (Ed.), Handbook of Optical Constants of Solids, Academic Press, San Diego, 1998.
[7] M.Q. Brewster, Thermal Radiative Transfer and Properties, John Wiley and Sons, New York, 1992.
[8] J. Nulman, S. Antonio, W. Blonigan, Observation of silicon wafer emissivity in rapid thermal processing chambers for pyrometric temperature monitoring, Appl. Phys. Lett. 56 (1990) 2513–2515.
[9] P. Vandenabeele, K. Maex, Influence of temperature and backside roughness on the emissivity of Si wafers during rapid thermal processing, J. Appl. Phys. 72 (1992) 5867–5875.
[10] P.J. Timans, Emissivity of silicon at elevated temperatures, J. Appl. Phys. 74 (1993) 6353–6364.
[11] G. Chen, T. Borca-Tasciuc, Photon effect on radiative properties of silicon during rapid thermal processing, J. Appl. Phys. 82 (1997) 830–835.